PROCEEDINGS A

rspa.royalsocietypublishing.org

Research

Check for updates

Article submitted to journal

Subject Areas:

Anisotropic elasticity, waves, meta-surfaces

Keywords:

Stroh formalism, surface waves, impact waves

Author for correspondence:

Yibin Fu

e-mail: y.fu@keele.ac.uk

THE ROYAL SOCIETY PUBLISHING

Reduced model for the surface dynamics of a generally anisotropic elastic half-space

Yibin Fu[1], Julius Kaplunov[1] and Danila Prikazchikov[1]

[1]School of Computing and Mathematics, Keele University, ST5 5BG, U.K.

Dedicated to the memory of Peter Chadwick, FRS

Near-surface resonance phenomena often arise in semi-infinite solids. For instance, when a moving load with a speed v close to the surface wave speed v_R is applied to the surface of an elastic half-space, it will give rise to a large-amplitude disturbance inversely proportional to $v - v_R$. The latter can be determined by a multiple-scale approach using an extra slow time variable. It has also been shown for isotropic elastic half-spaces that the reduced governing equation thus derived is capable of describing the surface wave contribution even for arbitrary dynamic loading. In this paper, we first derive the analogous evolution equation for a generally anisotropic elastic half-space, and then assess its applicability in the study of travelling waves in a half-space that is coated with a continuous array of spring-like vertical resonators or bonded to an elastic layer of different properties. Our results are validated by comparison with previously known results, and illustrative calculations are carried out for a fibre-reinforced half-space and a coated half-space that is subjected to a finite deformation.

1. Introduction

Mathematical modelling of near-surface wave fields is of major importance for numerous technical applications, including in particular non-destructive testing, reduction of ground vibrations induced by high-speed trains, and earthquake protection with a fresh interest in the design of seismic meta-surfaces (Colombi et al , 2016; Colquitt et al , 2017). It has also attracted attention due to its relevance in the design of smart surfaces and flexible electronic devices (Bigoni et al , 2008; Li et al , 2018; Rogers et al , 2010). A recent trend in the theory of surface waves is concerned with development of hyperbolic-elliptic asymptotic models that capture the contribution of surface waves to the overall dynamic response when surface tractions are prescribed (Kaplunov and Kossovich , 2004; Kaplunov et al , 2006). Within these formulations, the propagation of the Rayleigh wave is described by a hyperbolic equation along the surface (more precisely a forced wave equation), with decay into the interior governed by quasi-static elliptic equations. They are derived by perturbing the solution for the forced dynamic equations in linear elasticity around the eigensolution, corresponding to surface waves of arbitrary profile that have been studied by Sobolev (1937), Friedlander (1948), and Chadwick (1976) for the plane strain case, and recently extended by Kiselev and Parker (2010) to the 3D setup. We also mention extensions to anisotropy addressed in Achenbach (1998); Parker (2013); Prikazchikov (2013). The approach in Kaplunov et al (2006) was later adapted for a coated half-space (Dai et al , 2010). It also led to elegant explicit approximate solutions for the near-resonant regimes of a moving load on an elastic half-space, see Erbas et al (2017); Kaplunov and Prikazchikov (2013). A more systematic exposition of this methodology may be found in Kaplunov and Prikazchikov (2013, 2017). This approach is of obvious interest in the modelling of the aforementioned seismic meta-surfaces, due to drastic simplification coming from neglecting the contribution of bulk waves, which is usually not significant in analysing the near-surface dynamics. Some preliminary results have been reported in Ege et al (2018), dealing with the effect of an array of oscillators attached to the surface of an elastic half-space. At the moment, the hyperbolic-elliptic models for surface waves are known for isotropic media, with apparently the only exception of a recent contribution, Nobili and Prikazchikov (2018), that is restricted to a special type of orthorhombic symmetry, for which surface waves decay exponentially with no oscillations and are thus similar to those in the isotropic context. On the other hand, free harmonic surface waves have already been well-studied for a variety of crystal symmetries, see e.g. Farnell (1970), with the important issue of existence/uniqueness resolved by Stroh (1962), Barnett and Lothe (1974, 1985), and Chadwick and Smith (1977). However, treatment of Rayleigh waves caused by surface tractions appears to be far less straightforward. In this paper, we derive a reduced model for the surface dynamics of a generally anisotropic elastic half-space.

The rest of this paper is organised as follows. First, in Section 2 we present a brief summary of the state-of-the art of the surface wave theory, in particular the Stroh formalism and the method of surface impedance matrix, for a generally anisotropic half-space. Then, in Section 3 the hyperbolic equation for the surface displacement is derived, generalising the previously obtained ones for isotropic and orthotropic media. As in Kaplunov et al (2006), a slow-time perturbation procedure is employed, that yields the Rayleigh wave eigenform at leading order, and it is at the next order that we arrive at a hyperbolic equation for surface displacement by imposing a solvability condition. Section 4 contains a discussion of the obtained formulation, and its comparison with known results for isotropic and orthotropic media, including solution for the Lamb problem. As non-trivial applications of our reduced model, we next consider in Section 5 a simple meta-surface model that involves a half-plane subject to a periodic array of mass-spring oscillators. Illustrative numerical results are used to show that the reduced model can describe the dispersion curve accurately over a larger parameter regime than expected. Then in Section 6 we consider propagation of travelling waves in a coated elastic half-space that is also subjected to a finite deformation. It is shown that the problem may be reduced to one involving the coating layer only, and the branch of the dispersion curve associated with the Rayleigh type mode is well approximated by using the reduced model when the coating layer is much softer than the half-space. The paper is concluded in the final section with a summary and a discussion of possible extensions of the present study.

2. Summary of the surface wave theory

We consider a generally anisotropic elastic half-space defined by

$$0 < x_2 < \infty, \quad -\infty < x_1, x_3 < \infty$$

relative to a rectangular coordinate system with coordinates (x_i). Free surface waves are governed by the equation of motion

$$c_{ijkl} u_{k,lj} = \rho \ddot{u}_i, \quad 0 < x_2 < \infty, \tag{2.1}$$

the traction-free boundary condition

$$t_i \equiv -c_{i2kl} u_{k,l} = 0 \quad \text{on} \ \ x_2 = 0, \tag{2.2}$$

and the decay condition

$$u_k \to 0 \quad \text{as}\ x_2 \to \infty, \tag{2.3}$$

where c_{ijkl} are the elastic moduli, ρ is the density, u_i denotes the displacement vector field, and equation $(2.2)_1$ serves to define the traction vector field $\boldsymbol{t}$ with components t_i. Throughout this paper, we use a comma to signify partial differentiation, a superimposed dot to denote material time derivative, and we employ the summation convention on repeated indices.

To construct a surface wave solution, we first try a travelling-wave solution of the form

$$\mathbf{u} = \mathbf{a}\, \mathrm{e}^{\mathrm{i}kpx_2} \cdot \mathrm{e}^{\mathrm{i}k\theta}, \quad \theta = x_1 - vt, \tag{2.4}$$

where $k > 0$ is the wave number, v the speed, and the constant p and amplitude vector $\mathbf{a}$ are to be determined. On substituting (2.4) into (2.1), we find that p and $\mathbf{a}$ are determined by the matrix equation

$$\left(p^2 T + p(R + R^T) + Q^v I \right) \mathbf{a} = \mathbf{0}, \tag{2.5}$$

where I is the identity matrix, the superscript "T" denotes matrix transpose, and the components of the three matrices T, R, Q^v are defined by

$$T_{ik} = c_{i2k2}, \quad R_{ik} = c_{i1k2}, \quad Q^v_{ik} = c_{i1k1} - \rho v^2 \delta_{ik}. \tag{2.6}$$

Under the assumption that c_{ijks} satisfies the strong convexity condition, the values of p determined by (2.5) cannot be pure real when $v = 0$ and they will remain complex until $v = \hat{v}$ at which at least one pair of these values first become pure real. The $\hat{v}$ is usually referred to as the limiting speed (Chadwick and Smith , 1977) and surface waves with $v < \hat{v}$ are said to be subsonic. An elegant result in anisotropic elasticity is that a unique free-surface wave should normally exist except in some special cases (Barnett and Lothe , 1974).

To characterize the free-surface wave solution, we assume that $v < \hat{v}$ and denote by $p^{(1)}, p^{(2)}, p^{(3)}$ the three values of p with positive imaginary parts and $\mathbf{a}^{(1)}, \mathbf{a}^{(2)}, \mathbf{a}^{(3)}$ the associated solutions for $\boldsymbol{a}$. Then a general solution that satisfies the decay condition (2.3) is

$$\mathbf{u}=\left(\sum_{j=1}^{3}c_j\mathbf{a}^{(j)}\mathrm{e}^{\mathrm{i}kp^{(j)}x_2}\right)\mathrm{e}^{\mathrm{i}k\theta}=A\langle \mathrm{e}^{\mathrm{i}kpx_2}\rangle\,\mathbf{c}\,\mathrm{e}^{\mathrm{i}k\theta}, \tag{2.7}$$

where c_1, c_2, c_3 are constants,

$$A=[\mathbf{a}^{(1)},\mathbf{a}^{(2)},\mathbf{a}^{(3)}],\ \ \mathbf{c}=[c_1,c_2,c_3]^T,$$

and $\langle \mathrm{e}^{\mathrm{i}kpx_2}\rangle$ denotes the diagonal matrix

$$\mathrm{diag}\,\{\mathrm{e}^{\mathrm{i}kp^{(1)}x_2},\mathrm{e}^{\mathrm{i}kp^{(2)}x_2},\mathrm{e}^{\mathrm{i}kp^{(3)}x_2}\}.$$

The boundary condition (2.2) can be written as

$$\mathbf{t}\equiv-(R^T\mathbf{u}_{,1}+T\mathbf{u}_{,2})=0. \tag{2.8}$$

On substituting the general solution (2.7) into (2.8), we obtain $B\mathbf{c}=\mathbf{0}$, where

$$B=[\mathbf{b}^{(1)},\mathbf{b}^{(2)},\mathbf{b}^{(3)}]=R^TA+TA\langle p\rangle,\quad \mathbf{b}^{(j)}=(R^T+p^{(j)}T)\mathbf{a}^{(j)} \tag{2.9}$$

without summation over j, and $\langle p\rangle=\mathrm{diag}\,\{p_1,p_2,p_3\}$.

At this juncture, we introduce the surface-impedance matrix M (Ingebrigtsen and Tonning , 1969) through $\mathbf{t}=kM\mathbf{u}$ at $x_2=0$. It can then be deduced from (2.7) and (2.8) that

$$M=-\mathrm{i}BA^{-1}. \tag{2.10}$$

In terms of this matrix, the boundary condition $B\mathbf{c}=\mathbf{0}$ may be rewritten as

$$M\mathbf{d}=\mathbf{0},\quad \text{where } \mathbf{d}=A\mathbf{c}. \tag{2.11}$$

We remark that it is advantageous to use M instead of B. Among the many useful properties of M, we mention that M is Hermitian so that the secular equation det $M=0$ for the surface-wave speed is real even for the most general anisotropic material (Stroh , 1962). In the early studies on surface waves, it was not realized that the secular equation for the wave speed could always be written as a real equation, and as a result it was thought that existence of surface waves in anisotropic materials could only be exceptional; see, e.g., Farnell (1970). Also, all the eigenvalues of M are monotone decreasing functions of v (Barnett and Lothe , 1985). As a result, whenever a surface wave exists it is unique, which is a useful property when det $M=0$ is solved numerically.

The surface-impedance matrix also has many applications other than in the surface-wave theory; see, e.g., Fu (2005). There now exist very efficient methods for computing this matrix. Firstly, this matrix has an integral representation given by

$$M=\left(\int_0^{\pi}{T_\phi}^{-1}d\phi\right)^{-1}\left(\pi I-\mathrm{i}\int_0^{\pi}{T_\phi}^{-1}{R_\phi}^{\mathrm{T}}d\phi\right), \tag{2.12}$$

where

$$T_\phi=\cos^2\phi\,T-\sin\phi\cos\phi\,(R+R^{\mathrm{T}})+\sin^2\phi\,Q^v,$$
$$R_\phi=\cos^2\phi\,R-\sin^2\phi\,R^{\mathrm{T}}+\sin\phi\cos\phi\,(T-Q^v).$$

This integral representation was first derived by Barnett and Lothe (1973), and later re-derived by Mielke and Fu (2004) using a different procedure. Secondly, the surface-impedance matrix can also be computed with the aid of the matrix Riccati equation

$$(M-\mathrm{i}R)T^{-1}(M+\mathrm{i}R^{\mathrm{T}})-Q^v=0, \tag{2.13}$$

see Biryukov (1985), Mielke and Sprenger (1998), Fu and Mielke (2002). A new perspective on (2.12) and (2.13) has also recently been given by Norris and Shuvalov (2010) and Norris et al

(2013) in terms of the matrix sign function. Finally, when $x_3 = 0$ is a plane of material symmetry, this matrix has a simple and explicit expression (Destrade and Fu , 2006; Fu , 2005; Fu and Brookes , 2006).

A simple method for computing the surface-wave speed v and the corresponding M is as follows. Increase v gradually from $v = 0$ and at each step use (2.12) to evaluate M and hence $\det M$. As soon as $\det M$ changes sign, use the corresponding values of M and v as an initial guess and solve (2.13) and $\det M = 0$ to find M and v accurately. Such calculations can be carried out using, for instance, the software package *Mathematica* (Wolfram , 1991). Alternatively, we may solve (2.13) and $\det M = 0$ simultaneously with the use of the command *NSolve* on *Mathematica*. Although this gives multiple solutions, the solution that satisfies our requirements must be semi-positive definite and is unique (Fu and Mielke , 2002).

In the following, we assume that v_R has been determined as the unique solution of $\det M = 0$, M_0 denotes M evaluated at $v = v_R$, and $\mathbf{d}$ the corresponding normalized non-trivial solution of $(2.11)_1$ (so that $M_0\mathbf{d} = \mathbf{0}$ and $|\mathbf{d}|^2 = \mathbf{d} \cdot \bar{\mathbf{d}} = 1$). In the plane-strain case, M_0 must necessarily take the form

$$M_0 = \begin{pmatrix} m_1 & m_3 + \mathrm{i}m_4 \\ m_3 - \mathrm{i}m_4 & m_2. \end{pmatrix}. \tag{2.14}$$

We may then take

$$\mathbf{d} = \mathbf{g}/|\mathbf{g}|, \quad \text{where } \mathbf{g} = (-m_3 - \mathrm{i}m_4, m_1)^T. \tag{2.15}$$

With the use of $(2.11)_2$, the solution (2.7) may be written as

$$\mathbf{u} = \mathbf{u}(\theta, x_2, k) = A\langle \mathrm{e}^{\mathrm{i}kpx_2}\rangle\, A^{-1}\mathbf{d}\, \mathrm{e}^{\mathrm{i}k\theta}. \tag{2.16}$$

We observe that this solution is only valid for $k > 0$. When $k < 0$, we would need to use $\bar{p}_1, \bar{p}_2, \bar{p}_3$ in the construction of the general decaying solution (2.7), where an overbar denotes complex conjugation. As a result, when $k < 0$, we have

$$\mathbf{u}(\theta, x_2, k) = \bar{A}\langle \mathrm{e}^{\mathrm{i}k\bar{p}x_2}\rangle\, \bar{A}^{-1}\bar{\mathbf{d}}\, \mathrm{e}^{\mathrm{i}k\theta}. \tag{2.17}$$

It then follows that

$$\mathbf{u}(\theta, x_2, k) = \overline{\mathbf{u}(\theta, x_2, -k)}, \quad \text{for } k < 0, \tag{2.18}$$

and we remark that this rule of defining a k-dependent function when k is negative in terms of the same function when k is positive applies to all k-dependent functions in our subsequent analysis. To facilitate analysis later, we define a new vector function $\mathbf{z}$ through

$$\mathbf{z}(k, x_2) = A\langle \mathrm{e}^{\mathrm{i}kpx_2}\rangle\, A^{-1}\mathbf{d}, \quad \text{when } k > 0, \tag{2.19}$$

and observe that it satisfies the differential equation

$$T\frac{\partial^2 \mathbf{z}}{\partial x_2^2} + \mathrm{i}k(R + R^T)\frac{\partial \mathbf{z}}{\partial x_2} - k^2 Q^v \mathbf{z} = \mathbf{0}, \quad 0 < x_2 < \infty, \tag{2.20}$$

and the boundary condition

$$T\frac{\partial \mathbf{z}}{\partial x_2} + \mathrm{i}kR^T\mathbf{z} = \mathbf{0}, \quad x_2 = 0. \tag{2.21}$$

As remarked above, for $k < 0$ we have $\mathbf{z}(k, x_2) = \overline{\mathbf{z}(-k, x_2)}$.

We may also rewrite (2.19) in the form

$$\mathbf{z}(k, x_2) = \mathrm{e}^{-kx_2 E}\mathbf{d}, \tag{2.22}$$

where the matrix E is related to M by

$$E = -\mathrm{i}A\langle p\rangle\, A^{-1} = T^{-1}(M + \mathrm{i}R^T), \tag{2.23}$$

see Fu and Mielke (2002). On differentiating (2.13) with respect to v, we obtain

$$M'E + \bar{E}^T M' = -2\rho v_R I,$$

where M' denotes dM/dv evaluated at $v = v_R$, and hereafter all quantities dependent on v are also evaluated at $v = v_R$ unless otherwise stated. The solution of this Liapunov matrix equation is given by

$$M' = -2\rho v_R \int_0^\infty \mathrm{e}^{-s\bar{E}^T}\mathrm{e}^{-sE}ds,$$

from which we obtain

$$\bar{\mathbf{d}}\cdot M'\mathbf{d} = -2\rho v_R |k| \int_0^\infty \mathbf{z}(k, x_2)\cdot\mathbf{z}(-k, x_2)dx_2, \tag{2.24}$$

which will be used later.

For an isotropic elastic half-space, we introduce the notations

$$\kappa = \sqrt{\frac{\lambda + 2\mu}{\mu}}, \quad k_1 = \sqrt{1 - \frac{\rho v_R^2}{\lambda + 2\mu}}, \quad k_2 = \sqrt{1 - \frac{\rho v_R^2}{\mu}}, \tag{2.25}$$

which are obviously connected by the identity $(1 - k_2^2) = \kappa^2(1 - k_1^2)$. It can then be shown that $p_1 = \mathrm{i}k_1,\ p_2 = \mathrm{i}k_2$, and

$$A = \begin{pmatrix} 1 & -\mathrm{i}k_2 \\ \mathrm{i}k_1 & 1 \end{pmatrix}, \quad B = \mu\begin{pmatrix} 2\mathrm{i}k_1 & 1 + k_2^2 \\ -1 - k_2^2 & 2\mathrm{i}k_2 \end{pmatrix}, \tag{2.26}$$

$$m_1 = \frac{\mu k_1(1 - k_2^2)}{1 - k_1 k_2}, \quad m_2 = \frac{\mu(1 - k_2^2)k_2}{1 - k_1 k_2}, \quad m_3 = 0, \quad m_4 = \frac{\mu(k_2^2 - 2k_1 k_2 + 1)}{k_1 k_2 - 1}.$$

We then have

$$\det M = \frac{4k_1 k_2 - (1 + k_2^2)^2}{1 - k_1 k_2}, \tag{2.27}$$

and so the secular equation determining the surface wave speed v_R is given by $4k_1k_2 - (1 + k_2^2)^2 = 0$.

3. Reduced dynamic model

To motivate the following analysis, we first note that the inhomogeneous ordinary differential equation

$$\frac{d^2x}{dt^2} + \omega_0^2 x = \sin\omega t$$

governs the oscillation of a simple harmonic oscillator with natural frequency ω_0 that is forced to oscillate at frequency ω. The forced oscillation is given by $x = \sin\omega t/(\omega_0^2 - \omega^2)$, and when ω is close to ω_0, near-resonance occurs and the leading order term of the solution is given by

$$x = \frac{1}{2\omega_0\epsilon}\sin(\omega_0 t - \epsilon t), \quad \epsilon \equiv \omega_0 - \omega. \tag{3.1}$$

It is seen that the solution is of order $1/\epsilon$, and the solution evolves on two time scales, represented by t and ϵt, respectively; see Kaplunov and Prikazchikov (2017) for further details.

When a half-space is subjected to a surface load (e.g. a high speed train) that is travelling with a speed close to the surface wave speed, the induced surface displacement has a similar behaviour. More generally, when the surface of a half-space is subjected to an impact, it is expected that a surface wave front will result that corresponds to the surface wave residue when the Fourier transform is applied to solve the impact problem. The surface wave front will also evolve in a similar manner (Kaplunov et al , 2006). Thus, we now use the small positive parameter ϵ to characterize the distance from the surface wave front, and we introduce a slow time variable

$$\tau = \epsilon t,$$

so that under the transformation $(x_1, x_2, t) \to (\theta, x_2, \tau)$ where $\theta = x_1 \pm v_R t$, we have

$$\frac{\partial}{\partial x_1} = \frac{\partial}{\partial \theta}, \quad \frac{\partial}{\partial t} = \pm v_R \frac{\partial}{\partial \theta} + \epsilon \frac{\partial}{\partial \tau}, \quad \frac{\partial^2}{\partial t^2} = v_R^2 \frac{\partial^2}{\partial \theta^2} \pm 2 v_R \epsilon \frac{\partial^2}{\partial \theta \partial \tau} + \epsilon^2 \frac{\partial^2}{\partial \tau^2}.$$

For either wavefront, $\theta = x_1 - v_R t$ or $\theta = x_1 + v_R t$, the last relation may be replaced by

$$\frac{\partial^2}{\partial t^2} = v_R^2 \frac{\partial^2}{\partial \theta^2} + 2\epsilon \frac{\partial^2}{\partial t \partial \tau} + O(\epsilon^2).$$

We now assume that a surface traction $\mathbf{t}^{(0)}$ of order $O(1)$ is applied on $x_2 = 0$, and we look for an asymptotic solution of the form

$$\mathbf{u} = \frac{1}{\epsilon} \mathbf{u}^{(1)}(\theta, x_2) + \mathbf{u}^{(2)}(\theta, x_2) + O(\epsilon). \tag{3.2}$$

On substituting this expansion into (2.1) and (2.2), and equating the coefficients of ϵ^{-1} and ϵ^0, we obtain

$$T\mathbf{u}^{(1)}_{,22} + (R + R^T)\mathbf{u}^{(1)}_{,\theta 2} + Q^v \mathbf{u}^{(1)}_{,\theta\theta} = 0, \quad 0 < x_2 < \infty, \tag{3.3}$$

$$T\mathbf{u}^{(1)}_{,2} + R^T \mathbf{u}^{(1)}_{,\theta} = 0, \quad \text{on } x_2 = 0, \tag{3.4}$$

$$T\mathbf{u}^{(2)}_{,22} + (R + R^T)\mathbf{u}^{(2)}_{,\theta 2} + Q^v \mathbf{u}^{(2)}_{,\theta\theta} = 2\rho \mathbf{u}^{(1)}_{,t\tau}, \quad 0 < x_2 < \infty, \tag{3.5}$$

$$T\mathbf{u}^{(2)}_{,2} + R^T \mathbf{u}^{(2)}_{,\theta} = -\mathbf{t}^{(0)}, \quad \text{on } x_2 = 0. \tag{3.6}$$

The leading order problem (3.3) and (3.4) can be solved by Fourier transform. The solution is given by

$$\mathbf{u}^{(1)} = \frac{1}{2\pi} \int_{-\infty}^{\infty} \tilde{\mathbf{u}}^{(1)} \mathrm{e}^{\mathrm{i}k\theta} dk, \tag{3.7}$$

$$\tilde{\mathbf{u}}^{(1)} = \mathcal{F}[\mathbf{u}^{(1)}] \equiv \int_{-\infty}^{\infty} \mathbf{u}^{(1)} \mathrm{e}^{-\mathrm{i}k\theta} d\theta = f(k, \tau)\, \mathbf{z}(k, x_2), \tag{3.8}$$

where the unknown amplitude function $f(k, \tau)$ satisfies the condition $f(-k, \tau) = \overline{f(k, \tau)}$. Throughout this paper we use both $\mathcal{F}[g]$ and $\tilde{g}$ to denote the Fourier transform of a function g, which is defined by the equation with "$\equiv$" in (3.8).

To solve the second-order problem, we first apply Fourier transform to (3.5) and (3.6) to obtain

$$T\tilde{\mathbf{u}}^{(2)}_{,22} + \mathrm{i}k(R + R^T)\tilde{\mathbf{u}}^{(2)}_{,2} - k^2 Q^v \tilde{\mathbf{u}}^{(2)} = 2\rho \tilde{\mathbf{u}}^{(1)}_{t\tau}, \quad 0 < x_2 < \infty, \tag{3.9}$$

$$T\tilde{\mathbf{u}}^{(2)}_{,2} + \mathrm{i}kR^T \tilde{\mathbf{u}}^{(2)} = -\tilde{\mathbf{t}}^{(0)}, \quad x_2 = 0, \tag{3.10}$$

where $\tilde{\mathbf{t}}^{(0)} = \mathcal{F}[\mathbf{t}^{(0)}]$. We next form the dot product of the left hand side (LHS) of (3.9) with the mode function $\mathbf{z}(-k, x_2)$ defined by (2.19), and integrate the resulting expression from 0 to ∞.

By integrating by parts and making use of the fact that by definition $\mathbf{z}(-k,x_2)$ satisfies (2.20) and (2.21) with k replaced by $-k$, we obtain

$$\int_0^\infty \mathbf{z}(-k,x_2)\cdot \text{LHS of (3.9)}\, dx_2 = -\left\{\mathbf{z}(-k,x_2)\cdot\left(T\tilde{\mathbf{u}}^{(2)}_{,2}+\mathrm{i}kR^T\tilde{\mathbf{u}}^{(2)}\right)\right\}\Big|_{x_2=0}$$
$$= \mathbf{z}(-k,0)\cdot\tilde{\mathbf{t}}^{(0)}, \tag{3.11}$$

where in obtaining the second equation above use has been made of (3.10). On replacing the LHS of (3.9) in (3.11) by the right hand side of (3.9), we obtain

$$2\rho\int_0^\infty \mathbf{z}(-k,x_2)\cdot\tilde{\mathbf{u}}^{(1)}_{t\tau}dx_2 = \mathbf{z}(-k,0)\cdot\tilde{\mathbf{t}}^{(0)},$$

or equivalently,

$$2\rho\frac{\partial^2 f}{\partial t\partial\tau}\int_0^\infty \mathbf{z}(-k,x_2)\cdot\mathbf{z}(k,x_2)dx_2 = \mathbf{z}(-k,0)\cdot\tilde{\mathbf{t}}^{(0)}. \tag{3.12}$$

When $k>0$, we have

$$\mathbf{z}(k,x_2) = A\langle \mathrm{e}^{\mathrm{i}kpx_2}\rangle A^{-1}\mathbf{d},\quad \mathbf{z}(-k,x_2)=\overline{\mathbf{z}(k,x_2)} = \bar{A}\langle \mathrm{e}^{-\mathrm{i}k\bar{p}x_2}\rangle \bar{A}^{-1}\bar{\mathbf{d}}, \tag{3.13}$$

and so

$$\int_0^\infty \mathbf{z}(-k,x_2)\cdot\mathbf{z}(k,x_2)dx_2 = \frac{1}{k}N, \tag{3.14}$$

where

$$N = \int_0^\infty A\langle \mathrm{e}^{\mathrm{i}ps}\rangle A^{-1}\mathbf{d}\cdot\bar{A}\langle \mathrm{e}^{-\mathrm{i}\bar{p}s}\rangle \bar{A}^{-1}\bar{\mathbf{d}}ds. \tag{3.15}$$

When $k<0$, we have

$$\mathbf{z}(-k,x_2) = A\langle \mathrm{e}^{-\mathrm{i}kpx_2}\rangle A^{-1}\mathbf{d},\quad \mathbf{z}(k,x_2)=\overline{\mathbf{z}(-k,x_2)} = \bar{A}\langle \mathrm{e}^{\mathrm{i}k\bar{p}x_2}\rangle \bar{A}^{-1}\bar{\mathbf{d}},$$

and so

$$\int_0^\infty \mathbf{z}(-k,x_2)\cdot\mathbf{z}(k,x_2)dx_2 = -\frac{1}{k}N. \tag{3.16}$$

Combining (3.14) and (3.16), we obtain

$$\int_0^\infty \mathbf{z}(-k,x_2)\cdot\mathbf{z}(k,x_2)dx_2 = \frac{1}{|k|}N, \tag{3.17}$$

and (3.12) reduces to

$$2\rho N\,\frac{\partial^2 f}{\partial t\partial\tau} = |k|\mathbf{z}(-k,0)\cdot\tilde{\mathbf{t}}^{(0)}. \tag{3.18}$$

Denoting $\epsilon^{-1}\tilde{\mathbf{u}}^{(1)}(k,0,\tau)=\epsilon^{-1}f(k,\tau)\mathbf{z}(k,0)$ by $\tilde{\mathbf{v}}(k,\tau)$, which is the Fourier transform of the leading-order displacement filed, we then have

$$2\rho N\,\epsilon\frac{\partial^2\tilde{\mathbf{v}}}{\partial t\partial\tau} = |k|\mathbf{z}(k,0)(\mathbf{z}(-k,0)\cdot\tilde{\mathbf{t}}^{(0)}) = |k|\left\{\mathbf{z}(k,0)\otimes\mathbf{z}(-k,0)\right\}\tilde{\mathbf{t}}^{(0)}, \tag{3.19}$$

where "$\otimes$" denotes tensor product. Since according to (2.19), $\mathbf{z}(k,0)$ is equal to $\mathbf{d}$ when $k>0$ and $\bar{\mathbf{d}}$ when $k<0$, the above expression may be rewritten as

$$2\rho N\epsilon\frac{\partial^2\tilde{\mathbf{v}}}{\partial t\partial\tau} = \begin{cases} k(\mathbf{d}\otimes\bar{\mathbf{d}})\tilde{\mathbf{t}}^{(0)}, & \text{if } k>0,\\ -k(\bar{\mathbf{d}}\otimes\mathbf{d})\tilde{\mathbf{t}}^{(0)}, & \text{if } k<0.\end{cases} \tag{3.20}$$

We note that the tensor product $\mathbf{d}\otimes\bar{\mathbf{d}}$ in the above equation can be expressed in terms of the surface impedance tensor M_0, and we have

$$\mathbf{d}\otimes\bar{\mathbf{d}} = \frac{\bar{M}_0^c}{\mathrm{tr}\bar{M}_0^c}, \tag{3.21}$$

where $\bar{M}_0^c$ denotes the cofactor of $\bar{M}_0$ (or the adjugate of M_0 since $\bar{M}_0=M_0^T$) and tr $\bar{M}_0^c$ its trace. The trace is equal to the second principal invariant of M_0 and so is equal to the product of the non-zero eigenvalues of M_0. The above relation (3.21) follows from the fact that $\bar{M}_0^c$ satisfies the equations $\bar{M}_0^c M_0 = M_0 \bar{M}_0^c = 0$ and must necessarily be rank-one.

Writing

$$\mathbf{d} \otimes \bar{\mathbf{d}} = K_1 + \mathrm{i} K_2 \tag{3.22}$$

with K_1 and K_2 denoting the real and imaginary parts of the left hand side, we have

$$-\mathrm{i}(\mathbf{d} \otimes \bar{\mathbf{d}}) = K_2 - \mathrm{i}K_1, \quad \mathrm{i}(\bar{\mathbf{d}} \otimes \mathbf{d}) = K_2 + \mathrm{i}K_1,$$

and so equation (3.20) may be reduced to

$$\begin{aligned} 2\rho N \epsilon \frac{\partial^2 \tilde{\mathbf{v}}}{\partial t \partial \tau} &= (K_2 - \mathrm{i}\,\mathrm{sgn}(k) K_1)\, \mathrm{i}k\, \tilde{\mathbf{t}}^{(0)} \\ &= K_2 \mathcal{F}[\frac{\partial \mathbf{t}^{(0)}}{\partial x_1}] + \frac{1}{\pi} K_1 \mathcal{F}[\frac{1}{x_1}] \mathcal{F}[\frac{\partial \mathbf{t}^{(0)}}{\partial x_1}], \end{aligned} \tag{3.23}$$

where use has been made of the fact that

$$\mathcal{F}[\frac{1}{x_1}] = \text{p.v.} \int_{-\infty}^{\infty} \frac{1}{x_1} \mathrm{e}^{-\mathrm{i}kx_1} dx_1 = -2\mathrm{i} \lim_{a \to 0} \int_a^{\infty} \frac{\sin kx_1}{x_1} dx_1 = -\mathrm{i}\pi\, \mathrm{sgn}(k). \tag{3.24}$$

In the above equation, p.v. denotes "principal value".

On inverting (3.23), we obtain

$$2\rho N \epsilon \frac{\partial^2 \mathbf{v}}{\partial t \partial \tau} = K_2 \frac{\partial \mathbf{t}^{(0)}}{\partial x_1} + \frac{1}{\pi} K_1 \frac{1}{x_1} * \frac{\partial \mathbf{t}^{(0)}}{\partial x_1}, \tag{3.25}$$

where the star denotes integral convolution. In terms of the original variables, this takes the form

$$\frac{\partial^2 \mathbf{u}}{\partial t^2} - v_R^2 \frac{\partial^2 \mathbf{u}}{\partial x_1^2} = \frac{1}{\rho N} \left\{ K_2 \frac{\partial \mathbf{t}^{(0)}}{\partial x_1} + \frac{1}{\pi} K_1 \frac{1}{x_1} * \frac{\partial \mathbf{t}^{(0)}}{\partial x_1} \right\}. \tag{3.26}$$

This is the evolution equation that governs the leading-order surface elevation near the surface wave front.

4. Validation

To validate the above evolution equation, we now specialize to the case when the elastic half-space is isotropic. We have $m_3 \equiv 0$ and

$$K_1 = \begin{pmatrix} m_4^2 & 0 \\ 0 & m_1^2 \end{pmatrix}, \quad K_2 = \begin{pmatrix} 0 & -m_1 m_4 \\ m_1 m_4 & 0 \end{pmatrix}.$$

Thus, denoting the two components of $-\mathbf{t}^{(0)}$ by (P_1, P_2), we have

$$-K_2 \mathbf{t}^{(0)} = (-m_1 m_4 P_2, m_1 m_4 P_1)^T, \quad -K_1 \mathbf{t}^{(0)} = (m_4^2 P_1, m_1^2 P_2)^T.$$

If, for instance, $P_1 = 0$, we obtain from (3.26)

$$v_R^2 \frac{\partial^2 u_1}{\partial x_1^2} - \frac{\partial^2 u_1}{\partial t^2} = -\frac{m_1 m_4}{\rho N} \frac{\partial P_2}{\partial x_1}, \quad v_R^2 \frac{\partial^2 u_2}{\partial x_1^2} - \frac{\partial^2 u_2}{\partial t^2} = \frac{m_1^2}{\rho N \pi} \frac{1}{x_1} * \frac{\partial P_2}{\partial x_1}. \tag{4.1}$$

This may be compared with equation (98) in Kaplunov and Prikazchikov (2017), namely,

$$v_R^2 \frac{\partial^2 u_1}{\partial x_1^2} - \frac{\partial^2 u_1}{\partial t^2} = \frac{v_R^2 (1 - k_2^4)}{4\mu B} \frac{\partial P_2}{\partial x_1} \tag{4.2}$$

in the current notation, where

$$B = \frac{k_1}{k_2}(1 - k_2^2) + \frac{k_2}{k_1}(1 - k_1^2) - 1 + k_2^2.$$

To this end, we first compute

$$\frac{m_1 m_4}{N} = -\frac{k_1^2 k_2 (1-k_2^2)^2}{4k_1^3 + k_2(k_2^2-7)k_1^2 + k_2^3 + k_2}. \tag{4.3}$$

In view of $(2.25)_3$, the equivalence of $(4.1)_1$ and (4.2) then hinges on the validity of

$$\frac{m_1 m_4}{N} = -\frac{(1-k_2^2)(1-k_2^4)}{4B}.$$

The last identity is indeed valid because the difference of the two sides can be shown to be proportional to $4k_1k_2 - (1+k_2^2)^2$ which is zero; see (2.27).

Agreement with the result of Nobili and Prikazchikov (2018) for the orthorhombic case can be achieved by using the fact that in this case the m_3 in (2.14) is zero, and the other three components are given by (Fu and Mielke , 2002)

$$m_1 = \sqrt{c_{66}(c_{11}-\rho v^2) - \frac{c_{66}}{c_{22}}\left(\frac{c_{12}+c_{66}}{1+\gamma}\right)^2},$$

$$m_2 = \gamma \frac{c_{22}}{c_{66}} m_1, \quad m_4 = \frac{\gamma c_{12} - c_{66}}{1+\gamma}, \quad \gamma = \sqrt{\frac{c_{66}(c_{66}-\rho v^2)}{c_{22}(c_{11}-\rho v^2)}}. \tag{4.4}$$

As another validation of our general evolution equation (3.26), we now solve it subject to the boundary condition

$$\mathbf{t}^{(0)} = \delta(x_1)\delta(t)\mathbf{g},$$

where $\mathbf{g}$ is a constant vector.

Applying Fourier transform to (3.26), we obtain

$$\frac{\partial^2 \tilde{\mathbf{u}}}{\partial t^2} + v_R^2 k^2 \tilde{\mathbf{u}} = \frac{\mathrm{i}k}{\rho N}\left\{K_2 \mathbf{g}\delta(t) - \mathrm{i}\,\mathrm{sgn}(k)\delta(t)\, K_1 \mathbf{g}\right\}. \tag{4.5}$$

Both $\tilde{\mathbf{u}}$ and $\partial\tilde{\mathbf{u}}/\partial t$ are zero for $t<0$ due to causality. It then follows that

$$\tilde{\mathbf{u}}(k,0^+) = [\tilde{\mathbf{u}}]_{t=0^-}^{t=0^+} = 0,$$

$$\frac{\partial \tilde{\mathbf{u}}}{\partial t}(k,0^+) = \left[\frac{\partial \tilde{\mathbf{u}}}{\partial t}\right]_{t=0^-}^{t=0^+} = \frac{\mathrm{i}k}{\rho N}\left\{K_2\mathbf{g} - \mathrm{i}\,\mathrm{sgn}(k)\, K_1\mathbf{g}\right\},$$

where the second jump condition is obtained by integrating (4.5) from $t=0^-$ to $t=0^+$. On solving (4.5) for $t>0$ subject to the two conditions above, we obtain

$$\tilde{\mathbf{u}} = \frac{\mathrm{i}}{\rho N v_R}\left\{K_2\mathbf{g} - \mathrm{i}\,\mathrm{sgn}(k)\, K_1\mathbf{g}\right\}\sin(k v_R t),$$

$$= \frac{1}{2\rho N v_R}\left\{K_2\mathbf{g} - \mathrm{i}\,\mathrm{sgn}(k)\, K_1\mathbf{g}\right\}[\mathrm{e}^{\mathrm{i}k v_R t} - \mathrm{e}^{-\mathrm{i}k v_R t}]. \tag{4.6}$$

Fourier inverting the above expression with the use of the shifting property and the fact that $\mathcal{F}[\delta(x)] = 1$ and $\mathcal{F}[1/(\mathrm{i}\pi x_1)] = -\mathrm{sgn}(k)$, we obtain

$$\mathbf{u} = \frac{1}{2\rho N v_R}\left\{K_2\mathbf{g}\left[\delta(x_1+v_R t) - \delta(x_1 - v_R t)\right] + \frac{1}{\pi}K_1\mathbf{g}\left[\frac{1}{x_1+v_R t} - \frac{1}{x_1 - v_R t}\right]\right\}. \tag{4.7}$$

The part of this result that represents the right-travelling wavefront may be compared with equation (22) in Maznev and Every (1997) which is rewritten in the Appendix A as equation

(A3) in the current notation. Agreement then hinges on the establishment of the identity

$$\mathrm{Res}_{v=v_R} M^{-1}(v) = -\frac{K_1 + \mathrm{i}K_2}{2\rho v_R N}, \tag{4.8}$$

where Res stands for "residue". This identity can be established by noting that the left hand side is equal to

$$\bar{M}_0^c \, \mathrm{Res}_{v=v_R} \frac{1}{\det M(v)} = \frac{\bar{M}_0^c}{(\det M)'} = \frac{\bar{M}_0^c}{\mathrm{tr}(M' \bar{M}_0^c)} = \frac{\mathbf{d} \otimes \bar{\mathbf{d}}}{\bar{\boldsymbol{d}} \cdot M' \boldsymbol{d}} = -\frac{K_1 + \mathrm{i}K_2}{2\rho v_R N}, \tag{4.9}$$

where use has in turn been made of Jacobi's identity, (3.21), (3.22), (2.24), and (3.17), and the $(\det M)'$ denotes differentiation of $\det M(v)$ with respect v followed by evaluation at $v = v_R$.

To conclude this section, we point out a simple interpretation of the evolution equation (3.26). We observe that in the Fourier space equation (3.26) reduces to

$$-(v^2 - v_R^2) k \tilde{\boldsymbol{u}} = \frac{1}{\rho N}(K_1 + \mathrm{i}K_2) \tilde{\boldsymbol{t}}^{(0)},$$

which, upon the further use of (4.8), becomes

$$(v + v_R)(v - v_R) k \tilde{\boldsymbol{u}} = 2 v_R \lim_{v \to v_R} (v - v_R) M^{-1}(v) \tilde{\boldsymbol{t}}^{(0)}. \tag{4.10}$$

In consistency with the limit taken, this is equivalent to

$$(v - v_R) k \tilde{\boldsymbol{u}} = \lim_{v \to v_R} (v - v_R) M^{-1}(v) \tilde{\boldsymbol{t}}^{(0)}. \tag{4.11}$$

This is recognized to be the leading order expansion of

$$\tilde{\boldsymbol{t}}^{(0)} = k M(v) \tilde{\boldsymbol{u}}, \quad \text{or equivalently,} \quad k \tilde{\boldsymbol{u}} = M^{-1}(v) \tilde{\boldsymbol{t}}^{(0)}, \tag{4.12}$$

in the limit $v \to v_R$; see the definition of the surface impedance matrix M above (2.10).

5. A half-space coated with an array of resonators

As a non-trivial application of our reduced model, we now consider an array of flexible rods that are clamped to the surface of the half-space. The longitudinal oscillations of the rods due to harmonic forcing at the base are governed by

$$E \frac{\partial^2 w}{\partial x_2^2} - m \frac{\partial^2 w}{\partial t^2} = 0, \quad -H < x_2 < 0, \tag{5.1}$$

$$\frac{\partial w}{\partial x_2} = \frac{P \mathrm{e}^{\mathrm{i}\omega t}}{E h}, \quad x_2 = 0, \tag{5.2}$$

$$\frac{\partial w}{\partial x_2} = 0, \quad x_2 = -H, \tag{5.3}$$

where E, m, H and h denote the Young's modulus, mass, height and width of each rod, respectively, and $P\mathrm{e}^{\mathrm{i}\omega t}$ is the normal force exerted by the half-space.

It can easily be shown that for each vibration frequency ω, the above system admits a solution of the form

$$w = -\frac{P c_0}{E h \omega \sin \omega H / c_0} \cos \frac{\omega}{c_0}(x_2 + H) \, \mathrm{e}^{\mathrm{i}\omega t}, \tag{5.4}$$

where $c_0 = \sqrt{E/m}$. It then follows that at the interface $x_2 = 0$, we have

$$P \mathrm{e}^{\mathrm{i}\omega t} = -\frac{E h \omega}{c_0} \tan\!\left(\frac{\omega}{c_0} H\right) w. \tag{5.5}$$

We observe that values of ω that satisfy $\tan(\frac{\omega}{c_0} H) = 0$ are natural frequencies of each rod with both ends free, whereas values of ω that satisfy $\tan(\frac{\omega}{c_0} H) = \infty$ are natural frequencies of each rod with the end $x_2=-H$ free and the end $x_2=0$ fixed. At the latter frequencies, the half-space would behave as if it were clamped at the surface and no non-trivial solutions can exist since it is well-known that a clamped elastic half-space cannot support surface wave solutions. This implies that the surface resonators will necessarily give rise to band gaps. What remains to be done is to characterize where and how wide they are.

Focussing now on waves whose wavelength is much larger than the gap width a between the rods, we may assume that the above forces are continuously distributed over the surface with density $P/a\mathrm{e}^{\mathrm{i}\omega t}$. Thus, the effective traction boundary condition for the half-space is

$$\mathbf{t}^{(0)}=\frac{Eh\omega}{ac_0}\tan(\frac{\omega}{c_0}H)\,w\boldsymbol{e}_2,\quad \text{at } x_2=0, \tag{5.6}$$

where $\boldsymbol{e}_2$ is the basis unit vector in the x_2-direction.

If we look for a solution for the half-space of the form

$$\boldsymbol{u}=\boldsymbol{f}\mathrm{e}^{\mathrm{i}(kx_1-\omega t)}, \tag{5.7}$$

then continuity of displacement at $x_2=0$ implies that

$$\mathbf{t}^{(0)}=\frac{Eh\omega}{ac_0}\tan(\frac{\omega}{c_0}H)\,f_2\mathrm{e}^{\mathrm{i}(kx_1-\omega t)}\boldsymbol{e}_2,\quad \text{at } x_2=0. \tag{5.8}$$

On substituting (5.7) and (5.8) into the reduced model (3.26), we obtain, by equating the component in the x_2-direction, the dispersion relation

$$v_R^2k^2-\omega^2=\frac{\omega k\,\mathrm{sgn}(k)m_1^2Eh}{\rho Nc_0a}\tan(\frac{\omega}{c_0}H). \tag{5.9}$$

This asymptotic dispersion relation is expected to provide a good approximation for the exact dispersion relation near the surface wave front $\omega\approx v_Rk$. The exact dispersion relation can be obtained by first substituting (5.8) into $\mathbf{t}^{(0)}=kM\boldsymbol{u}$. This gives

$$m_{11}f_1+m_{12}f_2=0,\quad m_{21}f_1+m_{22}f_2=\frac{Eh\omega}{ac_0k}\tan(\frac{\omega}{c_0}H)\,f_2, \tag{5.10}$$

where m_{ij} are the components of M. Existence of a non-trivial solution then requires that

$$\frac{1}{m_{11}}\det M=\frac{Eh\omega}{ac_0k}\tan(\frac{\omega}{c_0}H). \tag{5.11}$$

On expanding the left hand side of this exact dispersion relation around $v=v_R$ where $m_{11}=m_1$ and making use of the result in (4.9) for $(\det M)'$, we obtain

$$\frac{2\rho v_RN}{m_1^2}(v_R-v)=\frac{Eh\omega}{ac_0k}\tan(\frac{\omega}{c_0}H). \tag{5.12}$$

This reduces to (5.9) if the left hand side of the latter equation is first factorized as $(\omega+v_Rk)(\omega-v_Rk)$ and then the ω in the first factor is replaced by v_Rk.

We now compare the performance of the asymptotic dispersion relation (5.9) against its exact counterpart (5.11). For numerical illustrations, we shall consider a representative fibre-reinforced material with moduli given by

$$\begin{aligned}c_{ijkl}&=\lambda\delta_{ij}\delta_{kl}+\mu_t(\delta_{ik}\delta_{jl}+\delta_{il}\delta_{jk})+\alpha(\delta_{ij}a_ka_l+a_ia_j\delta_{kl})+\beta a_ia_ja_ka_l\\&\quad+(\mu_l-\mu_t)(a_ia_k\delta_{jl}+a_ia_l\delta_{jk}+a_ja_k\delta_{il}+a_ja_l\delta_{ik}),\end{aligned} \tag{5.13}$$

with $\lambda,\alpha,\beta,\mu_t,\mu_l$ material constants and a_i the preferred direction; see e.g., Spencer (1984). These constants are related to the Young's moduli E_l, E_t and Poisson's ratio ν_{lt} through

$$E_l=\hat{\beta}-\frac{(\alpha+\lambda)^2}{\lambda+\mu_t},\quad E_t=\frac{4\mu_t\left(\hat{\beta}(\lambda+\mu_t)-(\alpha+\lambda)^2\right)}{\hat{\beta}(\lambda+2\mu_t)-(\alpha+\lambda)^2},\quad \nu_{lt}=\frac{\alpha+\lambda}{2(\lambda+\mu_t)},$$

rspa.royalsocietypublishing.org Proc R Soc A 0000000

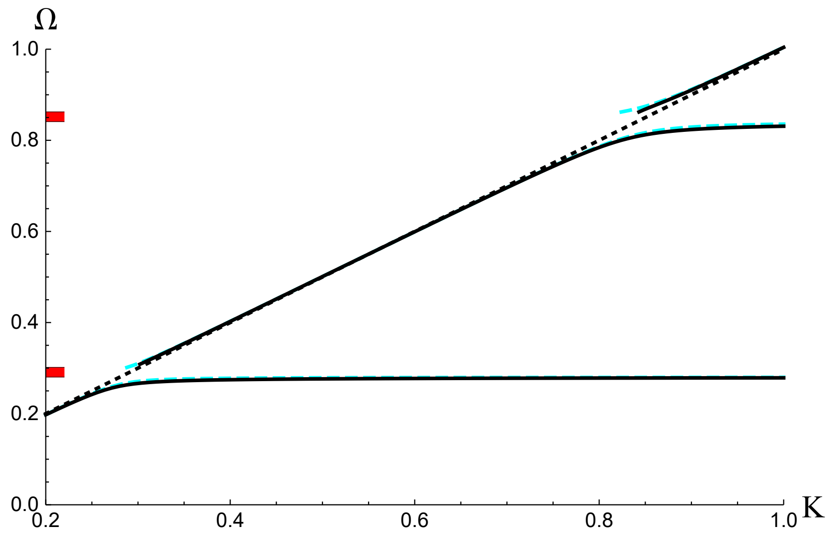

Figure 1. A typical dispersion curve when the fibres lie in the x_1x_2-plane and are parallel to the direction of wave propagation. The band gaps are marked on the Ω axis using rectangles. The solid and dashed lines represent the exact and asymptotic results, respectively, whereas the straight dotted line represents the surface wave line $\Omega = K$.

where $\hat{\beta} = \lambda + 2\alpha + 4\mu_l - 2\mu_t + \beta$. We shall take $\rho = 1852\,\mathrm{kg/m}^3$, $\nu_{lt} = 0.324$ and

$$(E_l,\ E_t,\ \mu_l,\ \mu_t) = (42.7,\ 11.6,\ 4.69,\ 6.07)\,\mathrm{GPa}, \tag{5.14}$$

given by Rikards et al (1999) for a typical Glass-Epoxy composite.

For the resonantors, we take

$$a = 2\mathrm{m}, \quad h = 0.3\mathrm{m}, \quad H = 14\mathrm{m}, \quad E = 1.7\,\mathrm{GPa}, \quad \rho_t = 450\mathrm{kg/m}^3.$$

We take $m_1 = \cos\phi$, $m_2 = \sin\phi$ with ϕ denoting the angle between the preferred/fibre direction (the l-direction) and the x_1-axis (the direction of wave propagation). We define

$$\Omega = \frac{a}{v_R}\omega, \quad K = ak,$$

so that the surface impedance matrix is a function of $v_R\Omega/K$. The surface wave front corresponds to $\Omega/K = 1$ and (subsonic) decaying waves can only exist for $v_R\Omega/K < \hat{v}$, that is

$$\frac{\Omega}{K} < \frac{\hat{v}}{v_R}, \tag{5.15}$$

where the limiting speed $\hat{v}$ is computed by using its definition (namely that it is the value of v at which at least one pair of values of p determined by (2.5) become pure real).

A typical set of results for the dispersion curve is shown in Figure 1, corresponding to $\phi = 0$. The solid black lines and dashed cyan lines represent the exact and asymptotic results, respectively, whereas the black dotted line represents the surface wave line $\Omega = K$. We make the following observations. First, the introduction of surface resonators gives rise to an infinite number of band gaps. For each band gap, the upper frequency limit corresponds to the intersection of the dispersion curve with the shear wave line $\Omega = (\hat{v}/v_R)K$ that is aways above the surface wave front $\Omega = K$. Except for the first branch that starts from the origin, each higher branch of the dispersion curve would initiate at the shear wave line and asymptote to a solution of $\tan(\omega H/c_0) = \infty$. This asymptotic limit defines the lower limit of each band gap. For the case considered in Figure 1, the first three band gaps are given by

$$(0.2803, 0.3017), \quad (0.8409, 0.8624), \quad (1.4015, 1.4230).$$

Second, although the asymptotic dispersion curve is only meant to be valid near the surface wave line, it is in fact also valid when the lower limit of each band gap is approached. This is due to the fact that this behaviour is dictated by $\tan(\omega H/c_0)$ tending to infinity, independent of the model describing the half-space. We do note, however, that although not shown in Figure 1, the asymptotic dispersion relation (5.9) admits solutions violating the restriction (5.15) which are clearly spurious. In other words, starting from the second branch, each cyan lines in Figure 1 could be extended leftwards and it would approach a solution of $\tan(\omega H/c_0) = \infty$ in the limit $K \to 0$. This corresponds to the fact that when $\tan(\omega H/c_0) \to \infty$, the two sides of (5.9) can be balanced in two different ways. The first way is to allow $K \to \infty$ (in which case both sides are infinite), as discussed earlier. The other way is to allow $K \to 0$ so that both sides remain finite.

We have also made calculations for a selection of values of ϕ between 0 and $\pi/2$. Qualitatively similar dispersion curves are obtained. For instance, for $\phi = \pi/3$, $\pi/4, \pi/2$, the first three band gaps are given by

$$\phi = \frac{\pi}{6}: \; (0.2779, 0.2635), \quad (0.8048, 0.7904), \quad (1.3318, 1.3173),$$

$$\phi = \frac{\pi}{4}: \; (0.2568, 0.2506), \quad (0.7581, 0.7519), \quad (1.2593, 1.2532),$$

$$\phi = \frac{\pi}{2}: \; (0.2918, 0.2830), \quad (0.8578, 0.8490), \quad (1.4237, 1.4149).$$

It is seen that the greatest and smallest band gaps are achieved at $\phi = 0$ and $\phi = \pi/4$, respectively. All the dispersion curves obtained here are also of the same structure as the one computed by Erbas et al (2017) for an isotropic half-space.

6. Dispersion relation for a coated half-space that is subject to a finite deformation

As another application of the reduced model (3.26), we now consider wave propagation in a coated elastic half-space that is subjected to a finite deformation. The equation of motion (2.1) is now replaced by its incremental counterpart

$$\chi_{ij,j} = \rho \ddot{u}_i, \quad \chi_{ij} \equiv \mathcal{A}^1_{jilk} u_{k,l}, \tag{6.1}$$

where $\mathcal{A}^1_{jilk}$ are the components of the first-order tensor of instantaneous elastic moduli given by

$$\mathcal{A}^1_{jilk} = \bar{J}^{-1} \bar{F}_{jA} \bar{F}_{lB} \left. \frac{\partial^2 W}{\partial F_{iA} \partial F_{kB}} \right|_{\mathbf{F}=\bar{\mathbf{F}}}. \tag{6.2}$$

See, e.g., Chadwick and Ogden (1971). In the above definition, W is the strain-energy function, F is the deformation gradient with $\bar{F}$ denoting its value corresponding to the finite deformation and $\bar{J} = \det \bar{F}$. We assume that the elastic half-space is defined by $0 < x_2 < \infty$ and the coating layer defined by $-h < x_2 < 0$ where h is the layer thickness in the finitely deformed configuration. For illustrative calculations, we assume that the strain-energy function is given by

$$W = \frac{\mu}{2}(I_1 - 2 - 2\log J) + \frac{\mu\nu}{1-2\nu}(J-1)^2, \tag{6.3}$$

where I_1 is the first principal invariant of $F^T F$, $J = \det F$, μ is the ground-state shear modulus, and ν is Poisson's ratio. The above strain energy function may be referred to as a *compressible neo-Hookean material model*. It recovers the classical neo-Hookean material model under the limit

$\nu \to \frac{1}{2}$, $J \to 1$ such that $(J-1)/(\nu - \frac{1}{2})$ remains finite. In the studies of wave propagation in pre-stressed media, it is customary to consider incompressible elastic materials to simplify analysis. To take advantage of the results presented in Sections 2 and 3, however, we find it more convenient to consider the above compressible material model and take the limit $\nu \to 1/2$ for the case of incompressibility. We assume that $\bar{F}$ corresponds to a plane-strain state of uni-axial compression in the x_1-direction with principal stretch λ. To simplify presentation further, we assume that the layer and half-space have the same density and Poisson's ratio and they only differ in their shear moduli $\hat{\mu}$ and μ. Correspondingly, the elastic moduli for the layer and half-space will be written as $\hat{\mathcal{A}}^1_{jilk}$ and $\mathcal{A}^1_{jilk}$, respectively.

It is straightforward to derive the dispersion relation for traveling waves in such a coated elastic half-space. We denote the displacement fields in the half-space and layer by $\boldsymbol{u}$ and $\hat{\boldsymbol{u}}$, respectively, and associated traction vectors by

$$t_i = -\mathcal{A}^1_{2ilk} u_{k,l}, \quad \hat{t}_i = \hat{\mathcal{A}}^1_{2ilk} u_{k,l}.$$

We look for a traveling-wave solution of the form

$$\boldsymbol{u} = \boldsymbol{z}(kx_2)\mathrm{e}^{\mathrm{i}k(x_1 - vt)}, \quad \hat{\boldsymbol{u}} = \hat{\boldsymbol{z}}(kx_2)\mathrm{e}^{\mathrm{i}k(x_1 - vt)}, \quad k > 0,$$

where the amplitude functions $\boldsymbol{z}(kx_2)$ and $\hat{\boldsymbol{z}}(kx_2)$ are to be determined. The conditions to satisfy are traction-free condition at $x_2 = -h$, displacement and traction continuity at the interface $x_2 = 0$ (namely, $\boldsymbol{u} = \hat{\boldsymbol{u}}$ and $\boldsymbol{t} = -\hat{\boldsymbol{t}}$), and decay condition as $x_2 \to \infty$. This problem can be reduced to a problem for the layer only, with the conditions at $x_2 = 0$ replaced by

$$-\hat{\boldsymbol{t}} = kM\hat{\boldsymbol{u}}, \tag{6.4}$$

where k and M have the same meanings as in (2.8)– (2.10) with c_{ijkl} there replaced by $\mathcal{A}^1_{jilk}$.

For the above traveling wave solution, the reduced model (3.26) reduces to

$$k(v_R^2 - v^2)\boldsymbol{u} = \frac{1}{\rho N}(K_1 + \mathrm{i}K_2)\boldsymbol{t}, \tag{6.5}$$

where we have replaced the leading-order traction vector $\boldsymbol{t}^{(0)}$ by $\boldsymbol{t}$. Displacement and traction continuity at $x_2 = 0$ implies that the above equation may be replaced by

$$k(v_R^2 - v^2)\hat{\boldsymbol{u}} = -\frac{1}{\rho N}(K_1 + \mathrm{i}K_2)\hat{\boldsymbol{t}}, \tag{6.6}$$

which provides an approximation for the exact relation (6.4). Recalling the interpretation in (4.10)–(4.12), we expect that it should provide a good approximation for the branch of the dispersion curve that is associated with the surface wave-type mode. This is verified in Figure 2 where we have shown the dispersion curves based on (6.4) (solid lines) and (6.6) (dashed line), respectively. The lowest branch is associated with a surface wave-type solution. The speed tends to the surface wave speed for the half-space in the limit $kh \to 0$, and to the shear wave speed for the layer in the limit $kh \to \infty$. The example corresponds to a modulus ratio $\mu/\hat{\mu} = 10$, that is the half-space is much harder than the layer. It is found that the approximate model (6.6) gives good results for high values of $\mu/\hat{\mu}$ and poor results when μ and $\hat{\mu}$ are comparable. Of course, when $\hat{\mu}$ becomes larger than μ, the surface wave-type mode ceases to exist, and then (6.6) becomes irrelevant.

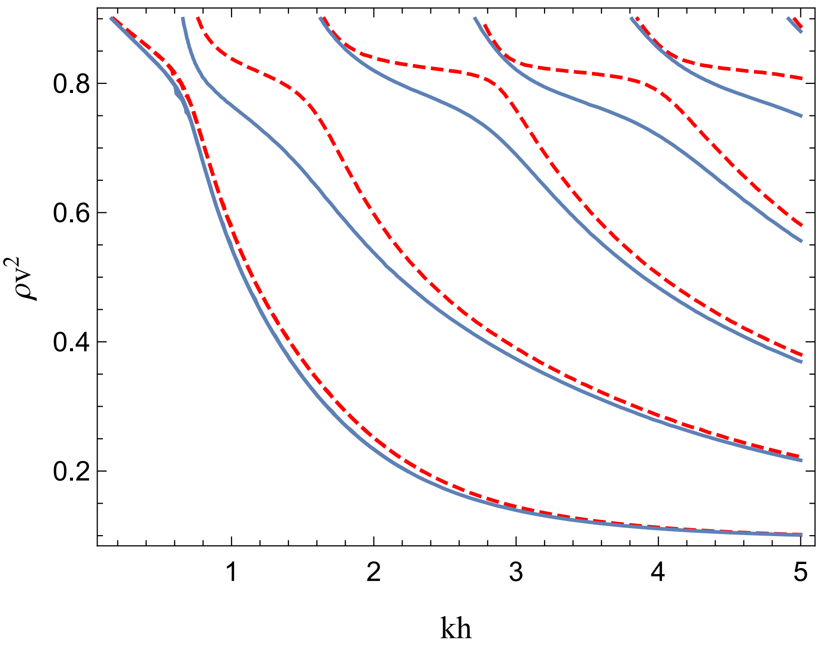

Figure 2. Dispersion curves for a traveling waves in a coated elastic half-space with principal stretch $\lambda = 1.01$, $\mu/\hat{\mu} = 10$ and $\nu = 0.4999$. Solid lines: exact results based on (6.4); dashed lines: approximate results based on the reduced model (6.4).

7. Conclusion

In this paper we have derived a forced wave equation governing the propagation of surface waves in a generally anisotropic elastic half-space due to prescribed surface loading. Although all the examples considered have simple enough exact solutions, it is hoped that our reduced model will be useful in other situations where the exact solutions are difficult to obtain or too involved to prevent easy interpretations. Also, since our forced wave equation may be viewed as the equation governing the forced oscillations of a string, it is possible that using this analogy expensive experiments involving a half-space may be carried out more cheaply on an analogous string.

Our reduced model extends what has previously been derived for isotropic and orthorhombic materials to the general anisotropic case. The method of derivation employed makes use of the surface impedance matrix and differs from the previously used method that depends on reducing the equation of motion to two scalar wave equations through the use of Helmholtz decomposition. Although we are dealing with the generally anisotropic case, the final results are quite compact and very easy to interpret; see, e.g., (4.10)–(4.12). Our reduced model also shares the same interpretations and extensions as discussed in Kaplunov and Prikazchikov (2017) for isotropic and orthorhombic materials. In particular, the surface wave front may be due to any form of time-dependant surface traction which appears on the right hand side of (3.26) as a forcing term; the only restriction being that the surface traction should indeed produce a surface wave front. We observe that although our derivation was presented as a leading-order analysis, the description of the surface wave front via (3.26) is in fact exact in the sense that if Laplace-Fourier transform is applied to the original dynamic problem and the inverse transform is evaluated to extract the surface displacement, then the contribution from the pole corresponding to the surface wave speed is exactly the same as what (3.26) would give. Although the reduced model is derived with a surface wave in mind, our last two examples concerning surface resonators and coated half-spaces serve to demonstrate that the reduced model may also apply to many other situations where surface wave type behaviour is involved. In particular, the recently considered problem for an isotropic half-space subject to an array of Euler-Bernoulli beams attached to the surface (Wootton et al , 2019) can be readily extended to the generally anisotropic case. Also the developed model may be implemented as a short-wave limiting behaviour in the composite hyperbolic equations for bending and extension of anisotropic strips, in a similar manner to what has been done earlier within the isotropic context (Erbas et al , 2018, 2019). The consideration in the paper is restricted to the surface. It is obvious that the general anisotropic case does not assume a simple solution for the interior domain, in contrast with the isotropic setup where the near-surface displacement field may be expressed through a single harmonic function (Kaplunov and Prikazchikov , 2017). However, with the use of the expressions (3.8) and (3.13) the near-surface field may still be obtained by evaluating a convolution integral. Finally, we mention that the presented 2D framework seemingly allows a 3D generalization by using the Radon transform as was done in (Kaplunov and Prikazchikov , 2017).

Appendix A: Exact solution of Lamb's problem for a generally anisotropic elastic half-space

It can be deduced from the summary in Section 1 that if

$$\mathbf{u}|_{x_2=0} = \mathbf{z}(0)\mathrm{e}^{\mathrm{i}(kx_1-\omega t)},$$

then the required surface traction is given by

$$\mathbf{t}|_{x_2=0} = |k| M(\frac{\omega}{k}) \mathbf{z}(0) \mathrm{e}^{\mathrm{i}(kx_1 - \omega t)},$$

where for $k<0$ the surface impedance matrix $M(\omega/k)$ should be replaced by its complex conjugate. We have not yet defined the surface impedance matrix for $|\omega/k| \geq \hat{v}$, but this is not required in the following calculation.

Let $\mathbf{z}(0) = |k|^{-1} M^{-1}(\omega/k)\mathbf{g}$, where $\mathbf{g}$ is an arbitrary column vector. Then

$$\mathbf{u}|_{x_2=0} = |k|^{-1} M^{-1}(\frac{\omega}{k})\, \mathbf{g}\, \mathrm{e}^{\mathrm{i}(kx_1-\omega t)}, \quad \Longleftrightarrow \quad \mathbf{t}|_{x_2=0} = \mathbf{g}\, \mathrm{e}^{\mathrm{i}(kx_1-\omega t)}.$$

This gives us the surface displacement when the surface traction is of the particular form given. Now suppose that the traction on the boundary is given by

$$\mathbf{t}|_{x_2=0} = \delta(x_1)\delta(t)\, \mathbf{g},$$

which may be rewritten as

$$\mathbf{t}|_{x_2=0} = \left(\frac{1}{4\pi^2} \int_{-\infty}^{\infty} dk \int_{-\infty}^{\infty} \mathrm{e}^{\mathrm{i}kx_1 - \mathrm{i}\omega t} d\omega \right) \mathbf{g}, \tag{A1}$$

then the associated surface displacement may be obtained by superposition as

$$\mathbf{u}|_{x_2=0} = \left(\frac{1}{4\pi^2} \int_{-\infty}^{\infty} dk \int_{-\infty}^{\infty} \frac{1}{|k|} M^{-1}(\frac{\omega}{k}) \mathrm{e}^{\mathrm{i}kx_1 - \mathrm{i}\omega t} d\omega \right) \mathbf{g}. \tag{A2}$$

The coefficient of $\mathbf{g}$ in the above expression is the surface Green's function with its ij-component giving the displacement in the i-th direction when $\mathbf{g}$ is the unit vector in the j-direction. Comparing this expression with equation (9) of Maznev and Every (1997) shows that their $\Phi(s)$ corresponds to our $\mathrm{i}vM^{-1}(v)$ with $s = 1/v$, and we have (with $s_R = 1/v_R$)

$$\mathrm{Res}_{s=s_R} \Phi(s) = \lim_{s \to s_R} (s - s_R)\Phi(s) = \lim_{v \to v_R} (\frac{1}{v} - \frac{1}{v_R}) \mathrm{i}vM^{-1}(v) = -\frac{\mathrm{i}}{v_R} \mathrm{Res}_{v=v_R} M^{-1}(v).$$

In terms of the surface impedance matrix, the equation (22) in Maznev and Every (1997) for the surface Green's function then takes the form

$$G(x,t) = \frac{1}{\pi} \,\mathrm{sgn}(x_1) \frac{\mathrm{Re}[\mathrm{Res}_{v=v_R} M^{-1}(v)]}{x_1 - v_R t} + \mathrm{Im}\,[\mathrm{Res}_{v=v_R} M^{-1}(v)]\, \delta(x_1 - v_R t), \tag{A3}$$

where the sign function $\mathrm{sgn}(x_1)$ may be deleted since the expression is only valid for the right-travelling surface wavefront where x_1 is necessarily positive.

Acknowledgements

We thank the referees for their constructive and insightful comments.

References

Achenbach, J. (1998). Explicit solutions for carrier waves supporting surface waves and plate waves. *Wave Motion* **28**, 89-97.

Barnett, D.M. and Lothe, J. (1973). Synthesis of the sextic and the integral formalism for dislocations, Greens function and surface waves in anisotropic elastic solids, *Phys. Norv.* **7**, 13-19.

Barnett, D.M. and Lothe, J. (1974). Consideration of the existence of surface wave (Rayleigh wave) solutions in anisotropic elastic crystals. *J. Phys. F: Metal Physics* **4**, 671-686.

Barnett, D.M. and Lothe, J. (1985). Free surface (Rayleigh) waves in anisotropic elastic half-spaces: the surface impedance method. *Proc. R. Soc. Lond.* A **402**, 135-152.

Bigoni, D., Gei, M. and Movchan, A.B. (2008). Dynamics of a prestressed stiff layer on an elastic half space: filtering and band gap characteristics of periodic structural models derived from long-wave asymptotics. *J. Mech. Phys. Solids* **56**, 2494-2520.

Biryukov, S.V. (1985). Impedance method in the theory of elastic surface waves. *Sov. Phys. Acoust.* **31**, 350-354.

Chadwick, P. (1976). Surface and interfacial waves of arbitrary form in isotropic elastic media. *J. of Elast.* **6**, 73-80.

Chadwick, P. and Ogden, R.W. (1971). On the definition of elastic moduli. *Arch. Ration. Mech. Anal.* **44**, 41-53.

Chadwick, P. and Smith, G.D. (1977). Foundations of the theory of surface waves in anisotropic elastic materials. *Adv. Appl. Mech.* **17**, 303-376.

Colombi, A., Roux, P., Guenneau, S., Gueguen, P., and Craster, R. V. (2016). Forests as a natural seismic metamaterial: Rayleigh wave bandgaps induced by local resonances. *Sci. rep.* **6**, 19238.

Colquitt, D. J., Colombi, A., Craster, R. V., Roux, P., and Guenneau, S. R. L. (2017). Seismic metasurfaces: Sub-wavelength resonators and Rayleigh wave interaction. *J. Mech. Phys. Solids* **99**, 379-393.

Dai, H.-H., Kaplunov, J., Prikazchikov, D. (2010). A long-wave model for the surface elastic wave in a coated half-space. *Proc. R. Soc. Lond.* A **466**, 3097-3116.

Destrade, M. (2007). Seismic Rayleigh waves on an exponentially graded, orthotropic half-space. *Proc. R. Soc. Lond.* A **463**, 495-502.

Destrade, M and Fu, Y.B. (2006). The speed of interfacial waves polarised in a symmetric plane. *Int. J. Eng. Sic.* **44**, 26-36.

Ege, N., Erbas, B., Kaplunov, J., Wootton, P. (2018). Approximate analysis of surface wave-structure interaction, *J. Mech. Mat. Struct.* **13**, 297-309.

Erbas, B., Kaplunov, J., Prikazchikov, D. A., Sahin, O. (2017). The near-resonant regimes of a moving load in a three-dimensional problem for a coated elastic half-space. *Math. Mech. Solids* **22**, 89-100.

Erbas, B., Kaplunov, J., Nolde, E., Palsu, M. (2018). Composite wave models for elastic plates. *Proc. R. Soc.* A **474**, 20180103.

Erbas, B., Kaplunov, J., Palsu, M. (2019). A composite hyperbolic equation for plate extension. *Mech. Res. Comm.* **99**, 64-67.

Farnell, G.W. (1970). Properties of elastic surface waves. In *Physical Acoustics* (ed. W.P. Mason and R.N. Thurston), 109-166. New York: Academic.

Friedlander, F. (1948). On the total reflection of plane waves. *Q. J. Mech. Appl. Maths* **1**, 376-384.

Fu, Y.B. (2005). An explicit expression for the surface-impedance matrix of a generally anisotropic incompressible elastic material in a state of plane strain. *Int. J. Non-linear Mech.* **40**, 229-239.

Fu, Y.B. and Brookes, D.W. (2006). An explicit expression for the surface-impedance tensor of a compressible monoclinic material in a state of plane strain. *IMA J. Appl. Maths* **71**, 434-445

Fu, Y.B. and Mielke, A. (2002). A new identity for the surface-impedance matrix and its application to the determination of surface-wave speeds. *Proc. R. Soc. Lond.* A **458**, 2523-2543.

Ingebrigtsen, K.A. and Tonning, A. (1969). Elastic surface waves in crystals. *Phys. Rev.* **184**, 942-951.

Kaplunov, Y. D., Kossovich, L. Y. (2004). Asymptotic model of Rayleigh waves in the farfield zone in an elastic half-plane. *Dok. Phy.* **49**, 234-236.

Kiselev, A., Parker, D. (2010). Omni-directional Rayleigh, Stoneley and Scholte waves with general time dependence. *Proc. R. Soc. Lond.* A **466**, 2241-2258.

Kaplunov, J., Prikazchikov, D. (2013). Explicit models for surface, interfacial and edge waves. In R. V. Craster, J. Kaplunov (Eds), *Dynamic localization phenomena in elasticity, acoustics and electromagnetism* (pp. 73-114). Wien: Springer.

Kaplunov, J., Prikazchikov, D.A. (2017). Asymptotic theory for Rayleigh and Rayleigh-type waves. *Adv. Appl. Mech.* **5**0, 1-106.

Kaplunov, J., Prikazchikov, D., Erbas, B., Sahin, O. (2013). On a 3D moving load problem for an elastic half space. *Wave Motion* **5**0, 1229-1238.

Kaplunov J, Zakharov A, Prikazchikov D. (2006). Explicit models for elastic and piezoelastic surface waves. *IMA J. Appl. Maths* **7**1, 768-782.

Li, G.-Y., Xu, G.Q., Zheng, Y. and Cao, Y.P. (2018). Non-leaky modes and bandgaps of surface acoustic waves in wrinkled stiff-film/compliant-substrate bilayers. *J. Mech. Phys. Solids* **1**12, 239-252.

Maznev, A.A. and Every, A.G. (1997). Time-domain dynamic surface response of an anisotropic elastic solid to an impulsive line force. *Int. J. Eng. Sci.* **3**5, 321-327.

Mielke, A. and Sprenger, P. (1998). Quasiconvexity at the boundary and a simple variational formulation of Agmon's condition. *J. Elast.* **51**, 23-41.

Mielke, A. and Fu, Y.B. (2004). Uniqueness of the surface-wave speed: A proof that is independent of the Stroh Formalism. *Math. Mech. Solids* **9**, 5-15.

Nobili, A., Prikazchikov, D.A. (2018). Explicit formulation for the Rayleigh wave field induced by surface stresses in an orthorhombic half-plane. *Eur. J. Mech. A/Solids* **7**0, 86-94.

Norris, A.N. and Shuvalov, A.L. (2010) Wave impedance matrices for cylindrically anisotropic radially inhomogeneous elastic materials. *Q. J. Mech. Appl. Math.* **6**3, 1-35.

Norris, A.N., Shuvalov, A.L. and Kutsenko, A.A. (2010) The matrix sign function for solving surface wave problems in homogeneous and laterally periodic elastic half-spaces. *Wave Motion* **5**0, 1239-1250.

Parker, D. (2013). The Stroh formalism for elastic surface waves of general profile. *Proc. R. Soc. Lond.* A **4**69, 20130301.

Prikazchikov, D. (2013). Rayleigh waves of arbitrary profile in anisotropic media. *Mech. Res. Comm.* **5**0, 83-86.

Rikards, R., Chatea, A., Steinchenb, W., Kesslerc, A. and Bledzkic, A.K. (1999). Method for identification of elastic properties of laminates based on experiment design. *Composites* B **3**0, 279-289.

Rogers, J.A., Someya, T. and Huang, Y.G. (2010). Materials and mechanics for stretchable electronics. *Science* **3**27, 1603-1607.

Sobolev, S. (1937). Some problems in wave propagation. In P. Frank and R. von Mises (Eds.), *Differential and integral equations of mathematical physics*. Russian translation (pp. 468-617). Moscow-Leningrad: ONTI.

Spencer, A.J.M. (1984). Constitutive theory for strongly anisotropic solids. In A.J.M. Spencer (Ed.), *Continuum Theory of the Mechanics of Fiber-Reinforced Composites*. CISM Courses and Lectures, No.**282**, pp. 1-32. Springer, Wien.

Stroh, A.N. (1958). Dislocations and cracks in anisotropic elasticity. *Phil. Mag.* **3**, 625-646.

Stroh, A.N. (1962). Steady state problems in anisotropic elasticity. *J. Math. Phys.* **4**1, 77-103.

Wolfram, S. (1991). *Mathematica: A System for Doing Mathematics by Computer (2nd Edn)*. Addison-Wesley, California.

Wootton, P., Kaplunov, J., Colquitt, D.J. (2019). An asymptotic hyperbolic-elliptic model for flexural-seismic metasurfaces. *Proc. R. Soc. Lond.* A **4**75, 20190079.